JB Accepted Manuscript Posted Online 3 February 2020
J. Bacteriol. doi:10.1128/JB.00541-19

Title

The ferric citrate regulator, FecR, is translocated across the bacterial inner membrane *via* a unique Twin-arginine transport dependent mechanism

Running Title

FecR insertion into the cytoplasmic membrane

Authors

Ian J Passmore[1], Jennifer M. Dow[1], Francesc Coll[1], Jon Cuccui[1], Tracy Palmer[2], Brendan W. Wren[1#]

[1]Department of Infection Biology, London School of Hygiene and Tropical Medicine, Keppel Street, London WC1E 7HT, UK

[2]Centre for Bacterial Cell Biology, Institute for Cell and Molecular Biosciences, Newcastle University, Newcastle upon Tyne, NE2 4HH, UK

Corresponding author

Email bredan.wren@lshtm.ac.uk

Abstract

In *Escherichia coli,* citrate-mediated iron transport is a key non-heme pathway for the acquisition of iron. Binding of ferric citrate to the outer membrane protein FecA induces a signal cascade that ultimately activates the cytoplasmic sigma factor FecI, resulting in transcription of the *fecABCDE* ferric citrate transport genes. Central to this process is signal transduction mediated by the inner membrane protein, FecR. FecR spans the inner membrane through a single transmembrane helix, which is flanked by cytoplasmic and periplasmic-orientated moieties at the N- and C- terminus. The transmembrane helix of FecR resembles a twin-arginine signal sequence, and substitution of the paired arginine residues of the consensus motif decouples the FecR-FecI signal cascade, rendering the cells unable to activate transcription of the *fec* operon when grown on ferric citrate. Furthermore, fusion of beta-lactamase C-terminal to the FecR transmembrane helix results in translocation of the C-terminal domain that is dependent on the twin-arginine translocation (Tat) system. Our findings demonstrate that FecR belongs to a select group of bitopic inner membrane proteins that contain an internal twin arginine signal sequence.

Importance

Iron is essential for nearly all living organisms due to its role in metabolic processes and as a cofactor for many enzymes. The FecRI signal transduction pathway regulates citrate-mediated iron import in many Gram-negative bacteria, including *Escherichia coli*. The interaction of FecR to outer membrane protein, FecA, and cytoplasmic anti-sigma factor, FecI, has been extensively studied. However, the mechanism by which FecR inserts into the membrane has not previously been reported. In this study, we demonstrate that targeting of FecR to the cytoplasmic membrane is dependent on the Tat system. As such, FecR

represents a new class of bitopic Tat-dependent membrane proteins with an internal twin arginine signal sequence.

Introduction

Iron is an essential element for virtually all organisms. Despite this, the toxicity, availability and solubility of iron present major challenges for bacteria, which require specialised iron transport systems. *Escherichia coli* K12 encodes two main non-heme pathways for the acquisition of iron from the environment. The first of these systems involves sequestering of iron *via* the siderophores enterobactin and ferrichrome that compete for Fe^{3+} bound to host proteins(1), whereas the second system involves ferric citrate uptake(2). Ferric citrate transport is mediated *via* the Fec system, which is comprised of a TonB-dependent outer membrane protein (FecA), a periplasmic-binding protein (FecB), inner-membrane proteins (FecCD) and ATPase (FecE)(3). The *fecABCDE* transport genes are induced upon detection of ferric citrate *via* the FecR-FecI signal cascade. FecR is an inner membrane protein with both periplasmic and cytoplasmic globular domains either side of a single trans-membrane helix(4). Binding of ferric citrate to FecA induces a conformational change, which is detected by the periplasmic C-terminal domain of FecR (Figure 1A). The signal is transduced across the membrane whereupon the cytoplasmic N-terminal face of FecR activates and releases the sigma factor FecI, which in turn recruits RNA polymerase to the *fec* operon(5, 6). Signal transduction across the inner membrane is central to this process and a number of key residues on the periplasmic and cytoplasmic domains of FecR have been identified as essential for interaction with FecA and FecI, respectively(7, 8). However, the mechanism by which FecR is inserted into the cytoplasmic membrane has not previously been reported.

Targeting of proteins to the bacterial cytoplasmic membrane occurs *via* the action of Sec machinery, the YidC insertase or the twin-arginine translocation (Tat) translocation pathway(9, 10). While most Tat substrates are soluble proteins released into the periplasm, a few substrates remain anchored in the cytoplasmic membrane, usually by an uncleaved N-terminal signal peptide, or a single C-terminal transmembrane helix(11–13). Whereas Sec exported proteins fold post-export, the Tat system exports proteins that have folded and matured in the cytoplasm. Tat substrates often contain complex cofactors and may co-export bound partner proteins, or are utilised by bacteria in extreme environments(14–16). However, some Tat substrates also include a number of monomeric, cofactor-less proteins, and for example, some halophilic archaea secrete the majority of their proteins *via* the Tat system, which may be an adaptive response to the fast-folding kinetics of proteins in a highly saline environment(17, 18).

Substrates are addressed to the Tat pathway *via* N-terminal signal peptides with a distinctive tripartite structure consisting of a basic n-region containing a conserved S/T-R-R-x-F-L-K “Tat motif”, a hydrophobic h-region, and a polar c-region harbouring the signal peptidase cleavage site(19). They frequently also contain one or more positive charges in the c-region that are not required for Tat transport but act as a Sec-avoidance motif(20, 21). Recently the polytopic Rieske protein of *Streptomyces coelicolor* was shown to be an unusual Tat substrate because it utilises the Sec machinery for insertion of its first two transmembrane helices and has an internal Tat signal sequence that forms the third transmembrane domain and that mediates export of the folded cofactor-containing domain across membrane(22, 23). Since this initial study, other families of polytopic inner membrane proteins that are simultaneously targeted to the Sec and Tat pathways have recently been described(21).

85 Here we demonstrate that FecR uses an internal Tat-targeting sequence for export of the 22
86 kDa C-terminal domain to the periplasm, whilst leaving a 9 kDa N-terminal domain in the
87 cytoplasm. This is the first example of a class of biotopic Tat-dependent membrane proteins
88 with an internal twin-arginine signal sequence.

89

90 **Results**

91 **An internal Tat-motif is conserved amongst FecR orthologues**

92 Previous studies have shown that *E. coli* K12 FecR spans the cytoplasmic membrane(4), but
93 the mechanism by which it is inserted into the bilayer has not been described. FecR does
94 not contain a classical signal sequence within its cytoplasmically orientated N-terminal
95 domain (residues 1-75). However, a twin-arginine motif with a good match to the Tat
96 consensus sequence immediately precedes a region of hydrophobicity that corresponds to
97 the transmembrane domain (Figure 1B). Both features are conserved characteristics of Tat
98 signal peptides. Similar to other Tat-dependent inner membrane proteins, FecR contains no
99 predicted cleavage site (Figure 1B). The amino acid sequences of putative FecR orthologues
100 derived from the eggNOG database(24) were aligned to assess conservation of this putative
101 Tat-targeting sequence (Figure S1). Out of the 95 predicted orthologues analysed, 93.7%
102 contained an internal twin-arginine motif. Those without Tat motifs were among those that
103 displayed the lowest sequence amino acid similarity to *E. coli* K12 FecR (Table S1) and
104 clustered independently from the other orthologues (Table S1, Figure S2A), suggesting that
105 these may not represent true FecR orthologues. Sequence motifs were generated using
106 Weblogo.3(25) with and without these outliers (Figure 1C and Figure S2B, respectively).
107 These alignments show clear conservation of the twin arginines, indicating that they may be

required for function. Furthermore, a high frequency of serine/threonine (-1 position), leucine (+3 position) and lysine residues (+4 position) was also noted, which are hallmarks of Tat signal sequences(26). FecR also contains two basic residues adjacent to the c-region that are known to act as Sec avoidance motifs (Figure 1B)(20, 21). This feature was also conserved amongst putative FecR orthologues (Figure 1D).

Periplasmic translocation of the FecR C-terminal domain is Tat-dependent

To determine whether membrane integration of FecR is dependent on the Tat export machinery, we constructed a fusion protein that could be deployed as a reporter for periplasmic translocation of the C-terminal domain (Figure 2A). The reporter FecR-BlaM was constructed by fusing the N-terminal domain and membrane-spanning region (amino acid residues 1-115) of *E. coli* FecR to β-lactamase (BlaM). This reporter was expressed under the transcriptional control of an arabinose inducible promoter in a *tat*$^{+}$ *E. coli* K12 strain (10β). β-lactamase fusions serve as ideal reporters for periplasmic export because they must be trafficked beyond the bacterial inner membrane to effectively protect the cell from β-lactam antibiotics. Furthermore, many β-lactamases can be translocated across the inner membrane *via* either Sec or Tat systems and are used as a reporter for both pathways(27, 28).

We assessed resistance to the β-lactam antibiotic ampicillin using M.I.C.Evaluator strips and by spotting serial dilutions on ampicillin plates (Figure S3). Table 1 and Figure 2B demonstrate that cells producing the FecR-BlaM reporter grew to a concentration of >256 μg ml^{-1}, indicating effective translocation of the β-lactamase to the periplasm. Removal of arabinose from the plate rendered this strain fully sensitive to ampicillin. To test whether the twin arginine motif was important for recognition of FecR by the Tat pathway, we

131 constructed substitutions of the arginine pair to twin alanine (radical) or twin lysine
132 (conservative). Cells producing the mutated fusion proteins demonstrated dramatically
133 increased sensitivity to ampicillin (MIC= 16 μg ml^{-1}) suggesting that almost no β-lactamase
134 had now been translocated to the periplasm. To further explore the Tat-dependence of this
135 fusion, the FecR-BlaM reporter was expressed in the Tat-deficient strain, HS3018-AΔ*tatABC*.
136 Consistent with the notion that insertion of the FecR transmembrane helix was Tat-
137 dependent, this strain demonstrated markedly increased ampicillin sensitivity relative to the
138 isogenic wild type (Figure 2C). Translation and membrane localisation of the fusion proteins
139 were not negatively affected by mutation of the twin-arginine motif or deletion of the Tat
140 system (Figure 3B and C), suggesting that ampicillin sensitivity was the consequence of
141 ineffective β-lactamase translocation.

142 **Mutation of the twin-arginine motif does not prevent membrane interaction**

143 Next, we determined whether substitutions of the paired arginine residues R79/80
144 influenced localisation of the FecR and the FecR-BlaM reporter (Figure 3A and B).
145 Comparison of the relative proportion of FecR and FecR-BlaM in the soluble (Figure 3A) and
146 membrane fractions (Figure 3B) revealed that the R79/80 substitutions did not prevent
147 membrane association of the proteins. We also expressed the FecR-BlaM reporter in the
148 wild type (HS3018-A) and *tat* mutant (HS3018-AΔ*tatABC*) strains (Figure 3C). Similarly, FecR-
149 BlaM localised to the membrane in the absence of a functional Tat system. To determine
150 whether FecR-BlaM was fully integrated into the bilayer, membranes of the wild type and
151 *tat* strains producing FecR-BlaM were washed with either 0.2M Na_2CO_3 or 4M urea (which
152 can displace peripheral membrane proteins by disrupting ionic interactions and disrupting
153 hydrogen bonding). Fig 3D shows that while carbonate washing had little effect on the

membrane localisation of FecR-BlaM in either strain, urea washing displaced FecR-BlaM from the membrane fraction of the *tat* mutant strain but not the wild type. These results confirm that FecR-BlaM behaves like an integral membrane protein in the wild type strain, but not is not correctly membrane integrated in the absence of the Tat machinery.

Mutation of the twin-arginine residues results in downregulation of the *fecABCDE* operon

No marked difference in growth rate was observed between HS3018-A and the *tat* mutant when grown with ferric citrate as a sole iron source (Figure S4), which is consistent with observations made by Ize *et al.,* 2004(29). Previous characterisation of the Fec system in *E. coli* has been performed using strains with an *aroB* mutation (*E. coli* strain AA93), which are unable to synthesise the siderophore enterobactin (which may compensate for the lack of Fec-mediated ferric iron import)(30, 31). Although these studies have been performed using different genetic backgrounds, these data indicate that some strains of *E. coli* K12 can acquire ferric citrate in the absence of functional FecR.

To explore whether *fecR* RR to KK mutation influenced recognition of ferric citrate in iron-limiting conditions, transcription of the *fecABCDE* genes was determined by qPCR analysis. A strain deficient in the *fecR* gene (*E. coli* strain BW25113) was complemented *in trans* with either wild-type *fecR* or *fecR R79-80K* substitution, which were grown in media supplemented with 2'2'-dipyridyl and 1 mM sodium citrate. Cells were harvested at early stationary phase and we observed no difference in final optical density between the strains tested, suggesting that the *fecR* mutant could grow using ferric citrate as a sole iron source.

We observed statistically higher expression of *fecABCD* (but not *fecE*) in the *fecR* mutant relative to the *fecR R79-80K,* indicating that there is low level of transcription of the *fec* genes in this strain. Crucially, we observed significantly increased expression of the

177 *fecABCDE* operon in strain complemented with wild type *fecR* relative to *fecR R79-80K* and
178 the *fecR* mutant (Figure 4). This is consistent with the notion that the arginine to lysine
179 mutation prevents periplasmic translocation of the C-terminal domain, which abrogates
180 FecR binding to citrate-loaded FecA and decouples the FecIR signal cascade.

181 **Discussion**

182 In this study we have addressed the membrane integration pathway for the bitopic
183 membrane protein FecR. Analysis of the transmembrane domain of FecR homologues
184 demonstrates that it is preceded by a conserved twin arginine motif, and that several
185 positive charges are located close to the C-terminal end, a feature which is known to act as a
186 Sec-avoidance motif. Consistent with this, replacement of the C-terminal extracellular
187 domain of FecR with beta-lactamase resulted in beta-lactamase translocation that was
188 dependent on both the twin arginines and the Tat pathway. The Tat system is known to
189 integrate several classes of membrane protein, including monotopic proteins that are
190 anchored by a single N- or C-terminal transmembrane domain, and polytopic proteins
191 where only the final transmembrane domain is Tat-dependent(13, 21, 22, 32, 33). FecR
192 constitutes a new class of bitopic Tat-dependent membrane proteins with an internal,
193 uncleaved twin arginine signal sequence that separates two globular domains.

194 The polytopic Rieske protein of *Streptomyces coelicolor,* which require concerted action of
195 Sec and Tat pathways for membrane integration, contains more than one transmembrane
196 helix and have an odd number of transmembrane helices before the twin arginine residues.
197 Given that FecR only contains a single helix, it seems unlikely that it is targeted to the
198 membrane by a similar dual-action mechanism. Our data indicate that FecR associates with
199 the membrane in the absence of a functional Tat system (Figure 3), which could suggest co-

operation with another pathway for its insertion. However, a study by Gray *et al.,* (2011) demonstrated that FecR membrane localisation was unperturbed in a *yidC* mutant(10). The *E. coli* Tat substrate, SufI, and some thylakoid proteins have been shown to bind to the membrane before interaction with the Tat or in the absence of functional Tat machinery(34–37). Although our data clearly demonstrate that FecR is a Tat substrate, we do not rule out the possibility that it targets to the membrane *via* another pathway.

The mechanism by which the Tat system recognises this internal signal sequence is unclear, but it should be noted that the related thylakoid Tat system is capable of translocating the substrate protein pOE17 even after deliberate fusion of a large polypeptide domain N-terminal to the Tat signal peptide(38). This indicates that integration of bitopic proteins is likely to be a common feature of the Tat pathway from different organisms.

Interestingly, some complex Tat substrates have signal peptides that contain greatly extended n-regions prior to the twin-arginine motif(39). Such extensions are almost invariably found on substrates that bind redox cofactors and/or partner proteins prior to export, and they appear to serve as binding sites for dedicated chaperones that co-ordinate folding and assembly(40–44). FecR is distinct from these Tat substrates since it does not contain any redox cofactor, and its signal sequence n-region is considerably longer than other Tat signal peptide n-regions. It is not clear why FecR should be a Tat substrate, although feasibly it may be energetically favourable for FecR to fold in the cytoplasm prior to transport through the Tat machinery. Alternatively, it is conceivable that the FecR N-terminal domain binds FecI, driving cytoplasmic folding before its integration into the membrane. In conclusion, FecR joins an expanding list of inner membrane proteins that contain a non-N-terminal Tat signal sequence.

223

224

225 **Materials and Methods**

226 **Strains and plasmids**

227 Bacterial strains and plasmids used in this study are listed in Tables S2 and S3 respectively.
228 The ampicillin resistance cassette of plasmid pEC415 was exchanged for a kanamycin
229 cassette by Gibson assembly (NEBuilder HiFi Assembly master mix, NEB) using the primers
230 pET28akanF/R (pET28a as template) and pEC415kanF/R (pEC415 as template) to generate
231 the plasmid pEC415K.

232 Plasmid pECfecR-blaM was constructed by Gibson assembly using the primers fecRF/fecRR
233 and pEC415KfecRF/pEC415KfecRR with *E. coli* genomic DNA and pEC415K as template.
234 Amino acid residues 79 and 80 were mutated from arginine to alanine or lysine using the
235 primers fecR R7980A F/ fecR R7980 R and fecR R7980K F/fecR R7980 R, respectively.

236 5'-phosphorylated primers fecR-blaM His F and R were used to introduce a C-terminal His-
237 tag into fecR-blaM and fecR-R7980K-blaM using pECfecR-blaM and pECfecR-R7980K-blaM as
238 templates, generating plasmid pECfecR-blaM-His and pECfecR-R7980K-blaM-His,
239 respectively. Similarly, primers fecR His F and R were used to generate C-terminally His-
240 tagged fecR using pECfecR and pECfecR R7980K as templates to generate pECfecR-His and
241 pECfecR R7980K-His.

242 **Growth conditions**

243 *E. coli* strains were cultured in LB broth or agar (Merck, Millipore) at 37^{o}C and
244 supplemented, when required, with 50 µg ml^{-1} kanamycin and 100 µg ml^{-1} ampicillin.

Susceptibility of the *E. coli* strains harbouring FecR-BlaM reporter to ampicillin was investigated by determining the Minimum Inhibitory Concentration (MIC) that prevented growth. Overnight cultures of each strain was diluted to OD_{600} 0.5 and a bacterial lawn was grown on LB plates (supplemented with kanamycin) by swabbing. M.I.C Evaluator strips (Oxoid) were placed on the plates, which were grown overnight at 37°C. Three independent replicates were performed and representative images are shown.

For transcript and growth kinetic analysis cells were grown at 37°C in Nutrient Broth (Merck) supplemented with 50 µM 2,2'-dipyridyl and 1 mM citrate.

Membrane extractions

E. coli cells harbouring the plasmid pECfecR-blaM were grown overnight at 37°C in media supplemented with 0.2% w/v L-arabinose and 50 µg ml^{-1} kanamycin. Cells were pelleted by centrifugation (3200 x*g*) and resuspended in 20 mM Tris-HCl (pH7.5), 200 mM NaCl. Cells were lysed using a FastPrep homogeniser (MPBio) and unlysed cells and large cell debris was removed by centrifugation (7000 x*g*). The resulting clarified lysate was pelleted by ultracentrifugation (1 hour 150,000 x*g*) to separate membrane and soluble fractions. Membrane pellets were resuspended in 50 mM Tris HCl (pH 7.5), 5 mM $MgCl_2$, 10% (v/v) glycerol.

For membrane interaction assays, cells were resuspended in 50 mM Tris HCl (pH 7.5), 10% (v/v) glycerol and lysed as described above. Crude lysate was treated with either 0.2M Na_2CO_3 or 4M urea for 1 hour, at 4°C, followed by ultracentrifugation at 150,000 x*g*. Membrane pellets were resuspended in 50 mM Tris HCl (pH 7.5), 5 mM $MgCl_2$, 10% (v/v) glycerol.

267 **Immunoblot analysis**

268 Total protein concentration of each sample was quantified by Bradford assay and
269 normalised to equal concentrations. Proteins were resolved by SDS-PAGE with Mini-
270 PROTEAN TGX Stain-Free gels (BioRad) and transferred to nitrocellulose membranes using
271 the iBlot 2 dry blotting system (ThermoFisher). Prior to transfer, gels were imaged using
272 BioRad ChemiDoc MP imaging system to determine total protein content loaded in each
273 well. Primary antibody, Mouse anti-6xHis (Invitrogen, UK, used at 1:10000 dilution), was
274 suspended in PBS and 0.1% (v/v) Tween 20 and incubated with the membrane for 1 hour.
275 Membranes were washed three times with PBS and incubated for 45 min with a secondary
276 goat anti-mouse IgG IRDye680 antibody (LI-COR Biosciences, UK, both at 1:10000 dilution).
277 Fluorescent signal was detected with the Odyssey LI-COR detection system (LI-COR
278 Biosciences, UK).

279

280 **qPCR**

281 Cells were grown to early stationary phase. All cells were harvested and stored in RNAlater
282 (Ambion) at 4^{o}C overnight. Cells were sedimented by centrifugation and RNA was extracted
283 using the Monarch Total RNA Miniprep kit (NEB) according to the manufacturer's
284 instruction. The resulting RNA was used as a template for reverse transcription and
285 conversion into cDNA using Superscript IV reverse transcriptase (Invitrogen). qPCR was
286 performed on the cDNA using Power SYBR green (Thermo) according to the manufacturer's
287 instructions, with 10 pmol of the appropriate primers (see Table S4). Amplification was
288 performed using an ABI PRISM 7500 real-time PCR system, and fluorescence data was
289 processed using SDS software (ABI). Relative gene expression was determined using *gyrA*

and *rpoS* as controls. Three independent biological replicates were performed for each strain and growth condition.

Bioinformatic analysis

Sequences of theoretical FecR orthologues were retrieved from the eggNOG database of orthologous groups and functional annotations(24). Sequence alignments were constructed using ClustlW and ESPript 3.0(45). Phylogenetic trees were generated using Interactive Tree of Life software(46). Weblogo sequence motifs were generated using weblogo3(25).

Acknowledgments

This work was supported by the Wellcome Trust grant number 102979/Z/13/Z.

Competing interests

The authors declare no competing interests.

References

1. Neilands JB. 1995. Siderophores: Structure and Function of Microbial Iron Transport Compounds. J Biol Chem 270:26723–26726.

2. Braun V, Braun M. 2002. Iron transport and signaling in Escherichia coli. FEBS Lett 529:78–85.

3. Staudenmaier H, Van Hove B, Yaraghi Z, Braun V. 1989. Nucleotide sequences of the fecBCDE genes and locations of the proteins suggest a periplasmic-binding-protein-dependent transport mechanism for iron(III) dicitrate in Escherichia coli. J Bacteriol 171:2626–2633.

4. Welz D, Braun V. 1998. Ferric citrate transport of Escherichia coli: functional regions of the FecR transmembrane regulatory protein. J Bacteriol 180:2387–2394.

5. Ochs M, Veitinger S, Kim I, Welz D, Angerer A, Braun V. 1995. Regulation of citrate-dependent iron transport of Escherichia coli: fecR is required for transcription activation by FecI. Mol Microbiol 15:119–132.

6. Kim I, Stiefel A, Plantör S, Angerer A, Braun V. 1997. Transcription induction of the ferric citrate transport genes via the N-terminus of the FecA outer membrane protein, the Ton system and the electrochemical potential of the cytoplasmic membrane. Mol Microbiol 23:333–344.

7. Stiefel A, Mahren S, Ochs M, Schindler PT, Enz S, Braun V. 2001. Control of the ferric citrate transport system of Escherichia coli: mutations in region 2.1 of the FecI extracytoplasmic-function sigma factor suppress mutations in the FecR transmembrane regulatory protein. J Bacteriol 183:162–170.

8. Enz S, Mahren S, Stroeher UH, Braun V. 2000. Surface Signaling in Ferric Citrate Transport Gene Induction: Interaction of the FecA, FecR, and FecI Regulatory Proteins. J Bacteriol 182:637–646.

9. Collinson I, Corey RA, Allen WJ. 2015. Channel crossing: how are proteins shipped across the bacterial plasma membrane? Philos Trans R Soc Lond, B, Biol Sci 370.

10. Gray AN, Henderson-Frost JM, Boyd D, Sharafi S, Shirafi S, Niki H, Goldberg MB. 2011. Unbalanced charge distribution as a determinant for dependence of a subset of Escherichia coli membrane proteins on the membrane insertase YidC. MBio 2.

11. Bachmann J, Bauer B, Zwicker K, Ludwig B, Anderka O. 2006. The Rieske protein from Paracoccus denitrificans is inserted into the cytoplasmic membrane by the twin-arginine translocase. FEBS J 273:4817–4830.

12. De Buck E, Vranckx L, Meyen E, Maes L, Vandersmissen L, Anné J, Lammertyn E. 2007. The twin-arginine translocation pathway is necessary for correct membrane insertion of the Rieske Fe/S protein in Legionella pneumophila. FEBS Lett 581:259–264.

13. Hatzixanthis K, Palmer T, Sargent F. 2003. A subset of bacterial inner membrane proteins integrated by the twin-arginine translocase. Mol Microbiol 49:1377–1390.

14. DeLisa MP, Tullman D, Georgiou G. 2003. Folding quality control in the export of proteins by the bacterial twin-arginine translocation pathway. Proc Natl Acad Sci USA 100:6115–6120.

15. Sanders C, Wethkamp N, Lill H. 2001. Transport of cytochrome c derivatives by the bacterial Tat protein translocation system. Mol Microbiol 41:241–246.

16. Rodrigue A, Chanal A, Beck K, Müller M, Wu LF. 1999. Co-translocation of a periplasmic enzyme complex by a hitchhiker mechanism through the bacterial tat pathway. J Biol Chem 274:13223–13228.

17. Thomas JR, Bolhuis A. 2006. The tatC gene cluster is essential for viability in halophilic archaea. FEMS Microbiol Lett 256:44–49.

18. Rose RW, Brüser T, Kissinger JC, Pohlschröder M. 2002. Adaptation of protein secretion to extremely high-salt conditions by extensive use of the twin-arginine translocation pathway. Mol Microbiol 45:943–950.

19. Stanley NR, Palmer T, Berks BC. 2000. The twin arginine consensus motif of Tat signal peptides is involved in Sec-independent protein targeting in Escherichia coli. J Biol Chem 275:11591–11596.

20. Bogsch E, Brink S, Robinson C. 1997. Pathway specificity for a delta pH-dependent precursor thylakoid lumen protein is governed by a “Sec-avoidance” motif in the transfer peptide and a “Sec-incompatible” mature protein. EMBO J 16:3851–3859.

21. Tooke FJ, Babot M, Chandra G, Buchanan G, Palmer T. 2017. A unifying mechanism for the biogenesis of membrane proteins co-operatively integrated by the Sec and Tat pathways. Elife 6.

22. Keller R, de Keyzer J, Driessen AJM, Palmer T. 2012. Co-operation between different targeting pathways during integration of a membrane protein. J Cell Biol 199:303–315.

23. Hopkins A, Buchanan G, Palmer T. 2014. Role of the twin arginine protein transport pathway in the assembly of the Streptomyces coelicolor cytochrome bc1 complex. J Bacteriol 196:50–59.

24. Huerta-Cepas J, Szklarczyk D, Forslund K, Cook H, Heller D, Walter MC, Rattei T, Mende DR, Sunagawa S, Kuhn M, Jensen LJ, von Mering C, Bork P. 2016. eggNOG 4.5: a

hierarchical orthology framework with improved functional annotations for eukaryotic, prokaryotic and viral sequences. Nucleic Acids Res 44:D286–D293.

25. Crooks GE, Hon G, Chandonia J-M, Brenner SE. 2004. WebLogo: a sequence logo generator. Genome Res 14:1188–1190.

26. Bagos PG, Nikolaou EP, Liakopoulos TD, Tsirigos KD. 2010. Combined prediction of Tat and Sec signal peptides with hidden Markov models. Bioinformatics 26:2811–2817.

27. Pradel N, Delmas J, Wu LF, Santini CL, Bonnet R. 2009. Sec- and Tat-Dependent Translocation of β-Lactamases across the Escherichia coli Inner Membrane. Antimicrob Agents Chemother 53:242–248.

28. McCann JR, McDonough JA, Pavelka MS, Braunstein M. 2007. β-lactamase can function as a reporter of bacterial protein export during Mycobacterium tuberculosis infection of host cells. Microbiology 153:3350–3359.

29. Ize B, Porcelli I, Lucchini S, Hinton JC, Berks BC, Palmer T. 2004. Novel Phenotypes of Escherichia coli tat Mutants Revealed by Global Gene Expression and Phenotypic Analysis. J Biol Chem 279:47543–47554.

30. Ochs M, Veitinger S, Kim I, Welz D, Angerer A, Braun V. 1995. Regulation of citrate-dependent iron transport of Escherichia coli: fecR is required for transcription activation by FecI. Mol Microbiol 15:119–132.

31. Härle C, Kim I, Angerer A, Braun V. 1995. Signal transfer through three compartments: transcription initiation of the Escherichia coli ferric citrate transport system from the cell surface. EMBO J 14:1430–1438.

392 32. Bachmann J, Bauer B, Zwicker K, Ludwig B, Anderka O. 2006. The Rieske protein from
393 Paracoccus denitrificans is inserted into the cytoplasmic membrane by the twin-
394 arginine translocase. FEBS J 273:4817–4830.

395 33. James MJ, Coulthurst SJ, Palmer T, Sargent F. 2013. Signal peptide etiquette during
396 assembly of a complex respiratory enzyme. Mol Microbiol 90:400–414.

397 34. Bageshwar UK, Whitaker N, Liang F-C, Musser SM. 2009. Interconvertibility of lipid- and
398 translocon-bound forms of the bacterial Tat precursor pre-SufI. Mol Microbiol 74:209–
399 226.

400 35. Musser SM, Theg SM. 2000. Characterization of the early steps of OE17 precursor
401 transport by the thylakoid DeltapH/Tat machinery. Eur J Biochem 267:2588–2598.

402 36. Shanmugham A, Wong Fong Sang HW, Bollen YJM, Lill H. 2006. Membrane binding of
403 twin arginine preproteins as an early step in translocation. Biochemistry 45:2243–2249.

404 37. Hou B, Frielingsdorf S, Klösgen RB. 2006. Unassisted Membrane Insertion as the Initial
405 Step in ΔpH/Tat-dependent Protein Transport. Journal of Molecular Biology 355:957–
406 967.

407 38. Fincher V, McCaffery M, Cline K. 1998. Evidence for a loop mechanism of protein
408 transport by the thylakoid Delta pH pathway. FEBS Letters 423:66–70.

409 39. Berks BC, Sargent F, Palmer T. 2000. The Tat protein export pathway. Mol Microbiol
410 35:260–274.

411 40. Oresnik IJ, Ladner CL, Turner RJ. 2001. Identification of a twin-arginine leader-binding
412 protein. Mol Microbiol 40:323–331.

413 41. Jack RL, Buchanan G, Dubini A, Hatzixanthis K, Palmer T, Sargent F. 2004. Coordinating
414 assembly and export of complex bacterial proteins. EMBO J 23:3962–3972.

415 42. Connelly KRS, Stevenson C, Kneuper H, Sargent F. 2016. Biosynthesis of selenate
416 reductase in Salmonella enterica: critical roles for the signal peptide and DmsD.
417 Microbiology (Reading, Engl) 162:2136–2146.

418 43. Dow JM, Gabel F, Sargent F, Palmer T. 2013. Characterization of a pre-export enzyme-
419 chaperone complex on the twin-arginine transport pathway. Biochem J 452:57–66.

420 44. Dow JM, Grahl S, Ward R, Evans R, Byron O, Norman DG, Palmer T, Sargent F. 2014.
421 Characterization of a periplasmic nitrate reductase in complex with its biosynthetic
422 chaperone. FEBS J 281:246–260.

423 45. Robert X, Gouet P. 2014. Deciphering key features in protein structures with the new
424 ENDscript server. Nucleic Acids Res 42:W320–W324.

425 46. Letunic I, Bork P. 2016. Interactive tree of life (iTOL) v3: an online tool for the display
426 and annotation of phylogenetic and other trees. Nucleic Acids Res 44:W242-245.

427

428 **Figures legends**

429 **Figure 1**

430 **A**- Schematic representation of FecR-mediated signal transduction. Binding of ferric citrate
431 to the outer membrane protein, FecA, initiates a signal that is transmitted across the
432 cytoplasmic membrane by FecR. **B**- Sequence alignment of the putative internal Tat motif of
433 FecR (residues 68-109) with the N-terminal Tat motif of TorA (residues 1-52), displayed on

434 the figure. The Tat motif is boxed in red, TorA cleavage site is boxed in orange. Region of
435 hydrophobicity/membrane spanning region indicated green. Positively charged residues
436 adjacent to the FecR c-region are indicated by arrows and putative Sec avoidance (which
437 correspond to weblogo shown in Figure 1D) boxed in purple. **C**- Consensus Tat sequence
438 motif of predicted FecR eggNOG-derived orthologues, excluding the six sequences that do
439 not contain a consensus twin-arginine motif. Amino acid position relative to the twin-
440 arginine motif is denoted below. **D-** Sequence alignment consensus logo of the c-region of
441 the predicted FecR eggNOG-derived orthologues. Charged amino acid residues are coloured
442 in blue.

443 **Figure 2**

444 Mutation of twin arginine residues inhibits periplasmic translocation of a FecR-BlaM fusion.
445 **A**- Domain architecture of the FecR-BlaM reporter. Ampicillin sensitivity of the FecR-BlaM
446 reporter with RR to AA and KK substitutions (*E. coli* strain, 10β) (**B**) and the FecR-BlaM
447 reporter expressed in a Tat-deficient strain (*E. coli* strain, HS3018-A and HS3018-AΔ*tatABC*)
448 (**C**) determined using M.I.C.Evaluator strips. Representative images of three biological
449 replicates are shown.

450 **Figure 3**

451 Cell localisation of FecR-Bla-His reporter and FecR-His with RR to KK substitutions (10β) (**A**
452 and **B**) or FecR-Bla-His expressed in a Tat-deficient strain (HS3018-AΔ*tatABC*) (**C**). Soluble
453 and membrane fractions were resolved by SDS-PAGE, transferred to nitrocellulose
454 membranes probed with an anti-6xHis antibody. All gels were imaged prior to transfer to
455 determine total protein loaded in each well (shown in lower panel). **A**- Soluble fractions,
456 Lane 1: FecR-Bla-His; lane 2: FecR-Bla-His R79/80A; lane 3: FecR-His; lane 4: FecR-His

457 R79/80K. **B**-Membrane fractions- Lane 1: FecR-Bla-His; lane 2: FecR-Bla-His R79/80A; lane 3:
458 FecR-His; lane 4: FecR-His R79/80K. **C**- Lane 1: HS3018-A FecR-Bla-His, soluble fraction; lane
459 2: HS3018-AΔ*tat* FecR-Bla-His, soluble; lane 3 HS3018-A FecR-Bla-His, membrane fraction;
460 lane 4: HS3018-AΔ*tat* FecR, FecR-Bla-His, membrane fraction. **D**- Crude cell extracts were
461 washed with either 0.2M Na_2CO_3 or 4M urea prior to membrane sedimentation. Lane 1:
462 HS3018-A FecR-Bla-His, membrane fraction, Na_2CO_3; lane 2: HS3018-AΔ*tat* FecR-Bla-His,
463 membrane fraction, Na_2CO_3; lane 3 HS3018-A FecR-Bla-His, membrane fraction, urea; lane
464 4: HS3018-AΔ*tat* FecR-Bla-His, membrane fraction, urea.

465 **Figure 4**

466 Relative gene expression of the *fecABCDE* operon and *fecR* in iron-limiting conditions.
467 Quantitative real time PCR of a *fecR* mutant (strain BW25113) expressing either wild type
468 *fecR* or *fecR R79/80K* substitution and an empty plasmid control was performed on
469 RNA/cDNA extracted from cell cultures grown in media supplemented with 2'2'-dipyridyl
470 and 1 mM sodium citrate. Error bars represent the standard deviation from mean derived
471 from three biological replicates.

472 **Table 1**

473 Effect of amino acid substitutions and a functional Tat system on periplasmic translocation
474 of the FecR-BlaM fusion and the ability to support growth on ampicillin. Determination of
475 M.I.C was performed in triplicate and representative images are shown in Figure 2.

Strain	**FecR-BlaM fusion variant**	**Mean ampicillin Minimum Inhibitory concentration (μg ml^{-1})**

10β	Wild type	>256
10β	R79A R80A	16 ± 0.0
10β	R79K R80K	16 ± 0.0
HS3018-A	Wild type	>256
HS3018-AΔ*tatABC*	Wild type	2 ± 0.0

476

477

Figure 1

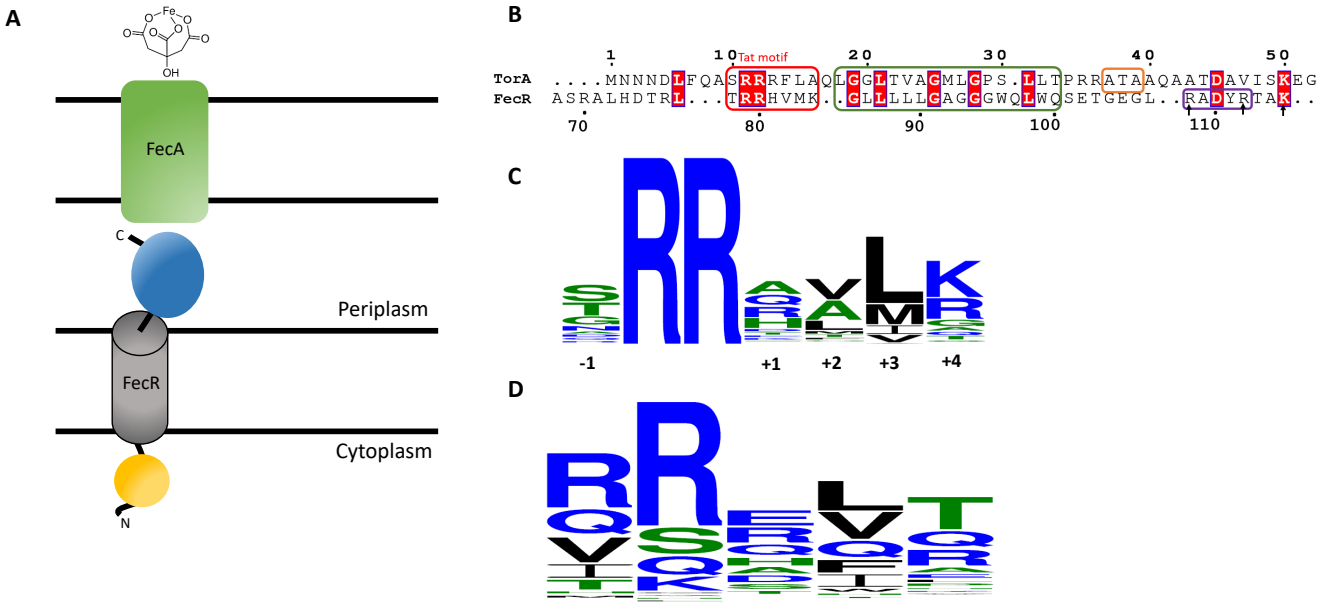

Figure 2

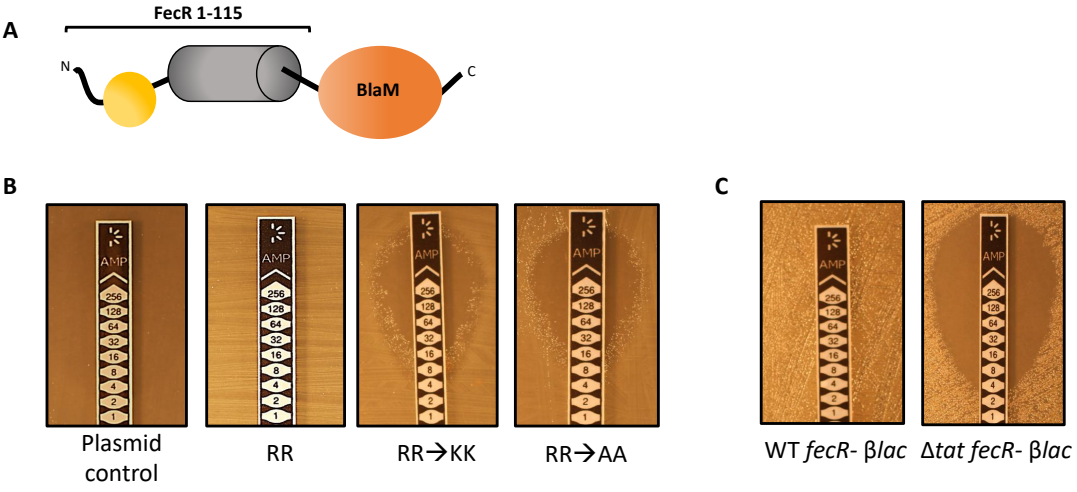

Figure 3

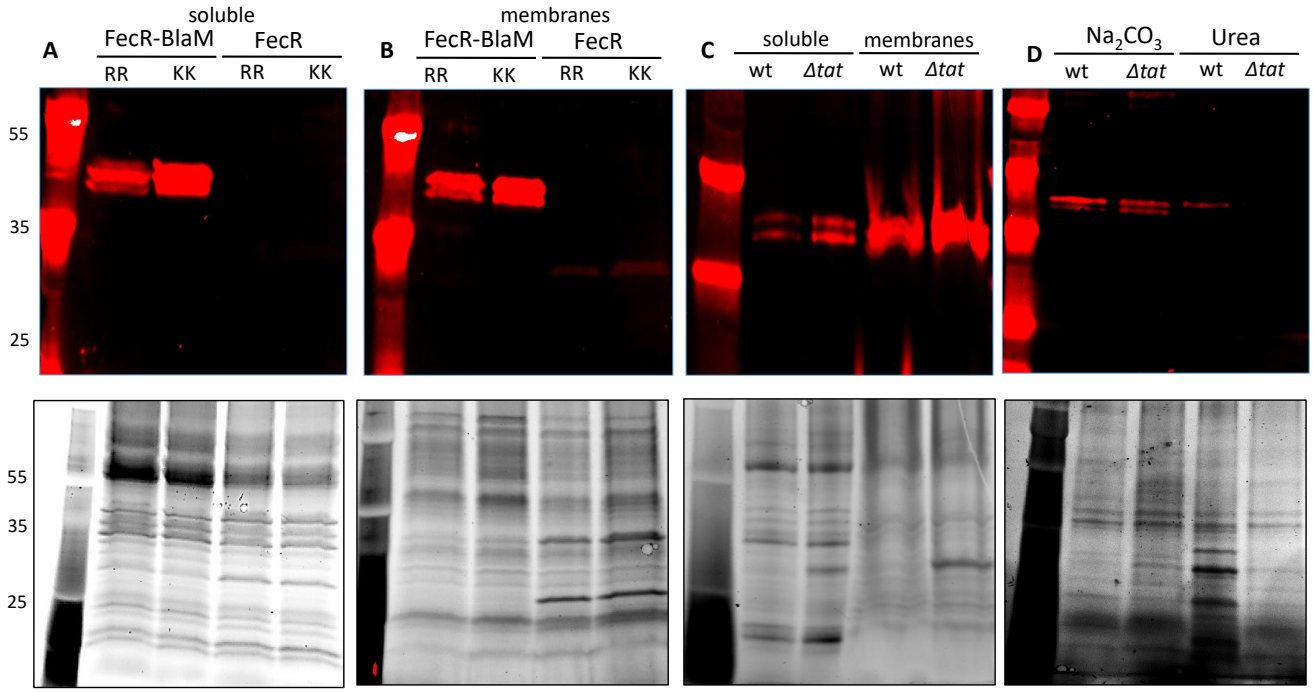

Figure 4